Versatile Boron Carbide–Based Energetic Time Delay Compositions

ARTICLE *in* ACS SUSTAINABLE CHEMISTRY & ENGINEERING · JULY 2013

Impact Factor: 4.64 · DOI: 10.1021/sc400187h

ACS Sustainable Chemistry & Engineering

Research Article

pubs.acs.org/journal/ascecg

Versatile Boron Carbide-Based Energetic Time Delay Compositions

Jay C. Poret, Anthony P. Shaw,* Christopher M. Csernica, Karl D. Oyler, Jessica A. Vanatta, and Gary Chen

Armament Research, Development and Engineering Center, U.S. Army RDECOM-ARDEC, Picatinny Arsenal, New Jersey 07806, United States

Supporting Information

ABSTRACT: Pyrotechnic time delay compositions composed of boron carbide, sodium periodate, and polytetrafluoroethylene have been developed for use in the U.S. Army hand-held signal. The new compositions were developed to replace the currently used composition that contains potassium perchlorate and barium chromate, chemicals that are facing increasing regulatory scrutiny. Static tests in aluminum hand-held signal delay housings demonstrated a wide range of available inverse burning rates (1.3−20.8 s/cm), which includes the 7−8.5 s/cm range required for hand-held signals. The roles of loading pressure, mixture stoichiometry, and component particle size are described herein.

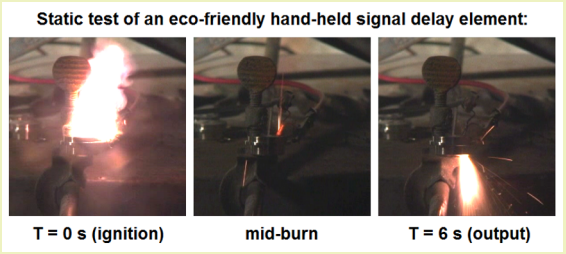

KEYWORDS: *Pyrotechnic delay, Boron carbide, Periodate, Hand-held signal, Sustainable chemistry*

INTRODUCTION

Pyrotechnic delays provide reproducible time intervals between energetic events. While electronic time delays are now used in advanced munitions, the simplicity and low cost of pyrotechnic delays is advantageous for inexpensive munitions such as hand grenades and signaling devices. Commonly used compositions include the tungsten delay ($W/BaCrO_4/KClO_4$/diatomaceous earth), manganese delay ($Mn/BaCrO_4/PbCrO_4$), zirconium−nickel delay (Zr−Ni alloy/$BaCrO_4/KClO_4$), and T-10 delay ($B/BaCrO_4$).[1−4] While these delay systems are effective and have been proven over many years of use, the heavy metals, chromates, and perchlorates they contain face increasing environmental scrutiny.[5−7]

Our research group is currently focused on developing environmentally benign replacement pyrotechnic compositions for U.S. Army hand-held signals.[8,9] In these devices, a pyrotechnic delay element provides the appropriate time interval for the signaling rocket to reach its apex before the pyrotechnic payload (illuminant or smoke) is expelled. The current HHS (hand-held signal) delay composition contains W, $BaCrO_4$, $KClO_4$, and VAAR (vinyl alcohol-acetate resin). Over the past three years, the U.S. Army's RDECOM Environmental Quality Technology Program has tasked our group to develop alternative delay compositions for HHS that do not contain any barium, chromates, or perchlorates. In our previous work, heat losses to the large pancake-shaped aluminum HHS housing caused many candidate compositions to extinguish, and only one system composed of W, Sb_2O_3, KIO_4, and calcium stearate was found to reliably give the desired long burning times (5−6 s, 7−8.5 s/cm).[10]

Although the antimony oxide in the $W/Sb_2O_3/KIO_4$/calcium stearate delay is arguably less hazardous than the $BaCrO_4$ it replaced,[11] antimony compounds remain a health and environmental concern.[12] A system free of antimony and containing fewer components was sought to mitigate future regulatory risk and to simplify the manufacturing process. We have now developed a versatile ternary system composed of B_4C, $NaIO_4$, and PTFE (polytetrafluoroethylene) to satisfy these objectives. Boron carbide, a hard ceramic material with a high melting point, was initially evaluated as a pyrotechnic fuel in the 1950s and 1960s but was not implemented in commercial or military pyrotechnics.[13−15] Recently, boron carbide has been rediscovered as a pyrotechnic fuel and has been tested in green light-emitting compositions.[16] Boron carbide-based compositions have also been demonstrated in environmentally benign white smoke grenades.[17,18] Moretti has proposed periodate salts (KIO_4, $NaIO_4$) as replacements for $KClO_4$ in flash/incendiary compositions,[19] and KIO_4 was chosen in lieu of $KClO_4$ during the development of the $W/Sb_2O_3/KIO_4$/calcium stearate delay.[10] Unlike perchlorate, periodate is not expected to compete with iodide in the thyroid gland due to its larger ionic radius.[20] PTFE is well known as a potent pyrotechnic oxidizer[21,22] and is also an excellent lubricant, allowing PTFE-based compositions to be pressed to very high consolidated densities with minimal loading force. While past PTFE manufacturing methods were criticized for the use of toxic PFOA (perfluorooctanoic acid) and related surfactants,[23] new methods that do not require these chemicals are being implemented.[24,25]

Received: June 19, 2013
Revised: July 8, 2013
Published: July 16, 2013

The performance of pyrotechnic delays is sensitive to many factors including component particle size, mixture stoichiometry, loading procedure, and housing configuration. Seemingly subtle differences in materials and methodology can cause noticeable (and sometimes profound) changes to the resulting delay times.[26−28] As a result, many military delay composition specifications are written broadly, and precise compositions are not assigned specific burning rates.[1,2,4] Instead, the key trends are mapped so that manufacturers can obtain the desired burning rate range while empirically adjusting for specific loading procedures and lot-to-lot differences in raw materials.

In this context, the $B_4C/NaIO_4$/PTFE system is a candidate for use in HHS delay elements, and the factors that influence its behavior must be critically examined. Herein, we describe the effects of loading pressure, mixture stoichiometry, and component particle size on the inverse burning rates and packing efficiencies of $B_4C/NaIO_4$/PTFE compositions. The *inverse* burning rate (IBR, s/cm) is the preferred performance metric for slow-burning delay compositions, as subtle differences in low rates are easily distinguished when the reciprocal rate data is plotted. Simple and rapid dry mixing methods produced compositions that burned reliably and reproducibly in the heavy aluminum HHS delay housing. Stable IBR ranging from 1.3 to 20.8 s/cm were achieved, encompassing the 7−8.5 s/cm range required for HHS. Furthermore, the compositions are readily ignited by black powder, a convenient and relatively low-temperature igniter[29] that is already used in HHS delay elements.

EXPERIMENTAL SECTION

Material Properties. Boron carbide powders (carbon rich, 19.0−21.7 wt % C) were obtained from AEE (Atlantic Equipment Engineers) and Alfa Aesar. Sodium periodate was obtained from Alfa Aesar and was separated into different fractions using U.S. mesh size 80, 200, and 325 screens. PTFE powders were obtained from AGC Chemicals and DuPont. For the sodium periodate fractions, a Malvern Morphologi G3S optical microscopy particle size analyzer was used to determine number-based circle-equivalent diameter distributions; volume-based distributions were calculated. For the boron carbide samples, a Microtrac S3500 laser diffraction particle size analyzer was used to determine volume-based diameter distributions of aqueous suspensions.

Preparation of Compositions and Delay Elements. The compositions are dry mixtures of two or three components. Small batches (3 g scale) were prepared by sealing the components in a conductive container and mixing with a Scientific Industries Vortex Genie vibrating shaker. Each composition was mixed for 3 min followed by visual inspection for large aggregates (which, if present, were broken with a spatula) followed by another 3 min of mixing. This protocol gave homogeneous compositions with consistent and reproducible IBR.

A Carver 3850 hydraulic press was used to load the compositions into aluminum HHS delay housings.[10] Unless otherwise specified, a dead load of 680 kg (376.6 MPa) was used for pressing. Black powder (class 7, 40−100 mesh) was used for the input and output charges. To prepare each delay element, 50 mg black powder was added and tamped, followed by the first half of the delay composition, and followed by pressing. Then, the second half of the delay composition was added and tamped, followed by 50 mg black powder, and followed by pressing.

For all of the experiments except the loading pressure study, the amounts of delay composition were chosen so that the total column lengths (including the input and output charges) were 9.4−10.2 mm long. For the loading pressure study, a fixed weight of delay composition was used, and the total column lengths varied from 9.1 to 9.8 mm. At 376.6 MPa, the input and output charges (the black powder) collectively occupied 2.8 mm of length in the cavity. This length did not change by more than 0.1 mm across the whole pressure range examined (251−502 MPa). Packing efficiency (as % TMD, the consolidated density as a percentage of theoretical maximum density) was calculated using 2.52, 3.86, and 2.3 g/cm^3 as the crystalline densities of B_4C,[30] $NaIO_4$,[31] and PTFE,[32] respectively.

Test and Analysis Protocols. Each finished delay element was held by a clamp with the small hole facing up. A small amount (20−30 mg) of loose black powder was placed on top of the small hole. This was ignited with an electrically heated nichrome wire. Digital video recordings, including those from a high-speed camera where appropriate, were used to measure the time between ignition of the input and first light of the output. Inverse burning rate (IBR, s/cm) was calculated by subtracting the burning time of the black powder layers (collectively 0.33 s) and then dividing the resulting time by the length of each delay column. Mass-based IBR (s/g) was calculated by dividing that time by the delay composition mass. The burning time of the black powder layers was the same at all loading pressures examined. Five delay elements were prepared and tested for each composition, and the results were averaged. The standard deviations of these measurements were generally less than 3%. Certain compositions close to a failure boundary exhibited erratic behavior, which is noted in the tables or in the text.

RESULTS AND DISCUSSION

Materials and Initial Experiments. Boron carbide is particularly attractive as a fuel for delay compositions because it has a substantially more positive heat of formation (−72 kJ/mol) than its oxides and a high melting point (2350 °C).[31,33] The former ensures enough heat will be generated to sustain the reaction in a small channel, while the latter allows the burning rate to be varied by small changes to the fuel particle size. Boron carbide remains in the solid state during oxidation, and the rate depends on surface area.[34] In this respect, boron carbide resembles tungsten, although unlike many delay compositions containing this fuel, boron carbide-based pyrotechnics are intrinsically gassy due to the volatility of the resulting oxides. Gassy delay compositions are acceptable for use in vented housings, such as the HHS delay housing. Additionally, as a ceramic material, boron carbide has a low thermal conductivity,[35] which is an important quality for slow-burning compositions where the rate of heat flow to subsequent layers in the burning column must be controlled.

Loose $B_4C/NaIO_4$ mixtures (B_4C = 10−20 wt %) were readily ignited with an electrically heated wire and produced clouds of purple smoke (presumably containing I_2). Burning W/KIO_4 mixtures are also known to emit purple smoke containing I_2.[10] These compositions are highly abrasive and easily bind the tooling used for pressing them into delay housings. Unlike $NaIO_4$, PTFE is both a pyrotechnic oxidizer and an excellent lubricant. In addition, PTFE is a thermal insulator, a factor that generally promotes slow burning rates. However, we were unable to ignite binary B_4C/PTFE mixtures as loose powders or as consolidated columns. Ternary $B_4C/NaIO_4$/PTFE mixtures may be consolidated in delay housings without difficulty due to the presence of the PTFE. These ternary mixtures ignited and propagated fully when consolidated in HHS delay housings. Ternary B_4C/KNO_3/PTFE mixtures also function in HHS delay housings, although they burn more quickly than their $NaIO_4$ analogues. As we are generally interested in achieving the lowest burning rates (highest IBR) possible, $NaIO_4$ was selected as the primary oxidizer for further investigations.

Loading Pressure and Packing Efficiency. Perhaps the easiest way to alter the burning rate of a pyrotechnic grain is to

vary loading force. Increased loading pressure usually results in greater packing efficiency (% TMD) and correspondingly less void space. In gassy systems, combustion gases migrate through void spaces ahead of the burning front, preheating unburnt layers and accelerating the overall linear burning rate.[36,37] Figure 1 shows the effect of varying loading pressure on a 15/75/10 mixture of $B_4C/NaIO_4$/PTFE. Both IBR and % TMD varied linearly over 251−502 MPa. IBR varied by ±10% about the center point (376.6 MPa, 4.89 s/cm), indicating a moderate sensitivity to changes in % TMD. The change in *mass-based* IBR (s/g) also followed the same trend. Indeed, all the linear IBR trends in this work agree with their mass-based analogues (Supporting Information). The linear metric, however, is of more practical significance.

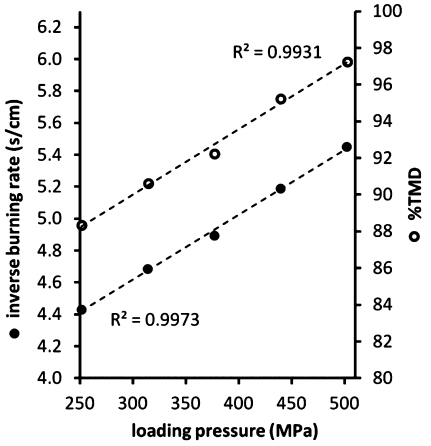

Figure 1. Inverse burning rate (s/cm, ●) and % TMD (○) as functions of loading pressure. Data is shown for a 15/75/10 mixture of $B_4C/NaIO_4$/PTFE. AEE 1500 grit B_4C, −325 mesh $NaIO_4$, and AGC FL1650 PTFE were used.

Composition Stoichiometry. Figure 2 shows changes to IBR and % TMD as a function of fuel level. In these compositions, the amounts of B_4C and $NaIO_4$ were varied, while PTFE was held constant at 10 wt %. IBR ranging from 1.27 s/cm (at 40 wt % B_4C) to 20.77 s/cm (at 8.75 wt % B_4C) were obtained. All the compositions plotted burned steadily with little variation in IBR between samples. Fuel-lean compositions containing 5 or 7.5 wt % B_4C failed to ignite and did not propagate. A very fuel-rich composition containing 60 wt % B_4C exhibited erratic behavior characterized by ignition failures, partial propagations, and high IBR variance for samples that did function (4.10 and 8.36 s/cm). Compositions with more than 60 wt % B_4C did not ignite.

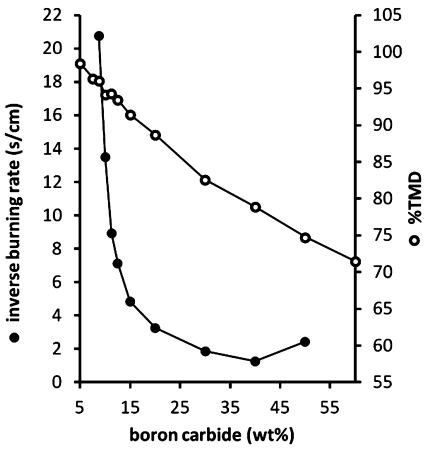

Figure 2. Inverse burning rates (s/cm, ●) and % TMD (○) for $x/(90 - x)/10$ mixtures of $B_4C/NaIO_4$/PTFE. Data is shown for compositions containing AEE 1500 grit B_4C, −325 mesh $NaIO_4$, and AGC FL1650 PTFE. All compositions were pressed at 376.6 MPa.

The hockey stick-shaped IBR curve in Figure 2 is similar to analogous plots for other systems such as the $W/BaCrO_4/KClO_4$/diatomaceous earth and $B/BaCrO_4$ delays.[1,4] Generally, at substoichiometric fuel levels the compositions exhibit both low exothermicity and low thermal conductivity, two complementary effects that give slow burning rates. While superstoichiometric fuel levels are also associated with low exothermicity, thermal conductivity generally increases with increasing fuel content. These two effects compete, and the IBR curves are therefore not as steep at the higher fuel levels.[38] For the compositions in Figure 2, packing efficiency is also affected by changes to boron carbide content. Even though the compositions were pressed at a constant loading pressure, % TMD decreased steadily as the B_4C level increased. As one of the hardest materials known, boron carbide is used extensively in industry as an abrasive, and this quality is not conducive to achieving high packing efficiencies. The IBR curve is therefore shaped by two effects: composition stoichiometry and packing efficiency. While this adds complexity to the physical interpretation of IBR trends, it is also important to know how composition changes affect packing efficiency. In production, delay columns are pressed at a fixed loading pressure, and packing efficiency is related to mechanical integrity.

With B_4C held constant at 15 wt %, the amounts of $NaIO_4$ and PTFE were varied (Figure 3). The binary $B_4C/NaIO_4$ composition burned at 3.13 s/cm, and the introduction of just 10 wt % PTFE increased this to 4.83 s/cm. Larger amounts of PTFE gave even larger increases in IBR until the compositions no longer ignited. Packing efficiency increased steadily as the PTFE level increased, a manifestation of this polymer's remarkable lubricating properties and tendency to deform under pressure. Delay columns containing large amounts of PTFE are both thermally insulated and effectively packed.

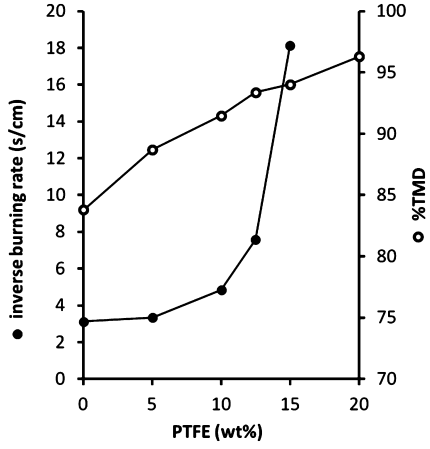

Figure 3. Inverse burning rates (s/cm, ●) and % TMD (○) for $15/(85 - x)/x$ mixtures of $B_4C/NaIO_4$/PTFE. Data is shown for compositions containing AEE 1500 grit B_4C, −325 mesh $NaIO_4$, and AGC FL1650 PTFE. All compositions were pressed at 376.6 MPa.

dx.doi.org/10.1021/sc400187h | ACS Sustainable Chem. Eng. 2013, 1, 1333−1338

These two factors promote slow burning rates until the combustion waves are no longer self-sustaining.

Component Particle Size and Type. The burning rates of boron carbide-based pyrotechnics are expected to be highly sensitive to variations in the fuel particle size. Table 1 shows particle size data for various B_4C samples. These samples were used to make delay elements with 15/75/10 and 20/70/10 mixtures of $B_4C/NaIO_4$/PTFE. As expected from the fuel level study (Figure 2), the compositions containing 15 wt % B_4C burned more slowly and had slightly greater packing efficiencies than their 20 wt % analogues (Table 2). Within each set of experiments, % TMD varied little, and the differences in IBR may be attributed to the different B_4C particle sizes. Delays containing fine B_4C (entries 1a−3a and 1b−3b) burned rapidly, while those containing coarser fuel burned much more slowly. Even though the B_4C samples varied by only 8−10 μm, the resulting IBR varied by more than 6-fold.

Table 1. Particle Size Data for B_4C Samples

type (lot)	$D[4,3]^a$	$D[v, 0.1]^b$	$D[v, 0.5]^b$	$D[v, 0.9]^b$
Alfa Aesar	5.35	1.59	5.02	8.77
AEE 1500 grit	5.09	1.79	4.64	8.99
AEE 1200 grit	5.19	1.82	4.69	9.16
AEE 800 grit (A)	16.62	2.54	9.24	36.74
AEE 800 grit (B)	14.12	7.87	13.71	20.23
mixture[c]	11.25	2.72	9.72	20.46

[a]Volume-based mean diameter in μm. [b]$D[v, x]$ is the diameter in μm that $(100 \times x)$% of the volume distribution is below. [c]A 50:50 mixture of Alfa Aesar and AEE 800 grit (B).

The IBR are better correlated with the amount of B_4C *fines* than with particle size mean (compare the mean and 10th percentile values in Table 1 with the results in Table 2). The most striking example is provided by the two different lots of "800 grit" B_4C. Here, the (A) lot has a distinctly greater mean but much more fine material as indicated by the lower $D[v, 0.1]$ value. Delay elements made with this lot burned much more rapidly than those made with the (B) lot. The amount of coarse particles as indicated by $D[v, 0.9]$ does matter but to a lesser degree. A mixture of the coarsest and finest B_4C samples gave material comparable to the 800 grit (A) lot. This mixture had a similar amount of fines but substantially fewer coarse particles than the (A) lot and therefore gave slightly faster-burning delay columns.

In contrast to the great sensitivity to B_4C particle size described above, variations in $NaIO_4$ and PTFE particle size have a smaller effect on inverse burning rate (see Supporting Information for detailed data tables). Commercially obtained $NaIO_4$ had a broad particle size distribution and was separated into fractions by screening. These fractions were used to prepare delay elements with 15/75/10 and 20/70/10 mixtures of $B_4C/NaIO_4$/PTFE. Despite a 3-fold difference in particle size between the finest and coarsest fractions (52 μm versus 150 μm), the resulting inverse burning rates varied by only 30%. As expected, the compositions containing finer $NaIO_4$ burned more rapidly.

PTFE is commercially available in various particle sizes and morphologies. Samples from AGC Chemicals had relatively high bulk densities and consisted mainly of rounded particles, while DuPont 7C had a much lower bulk density due to its extremely fibrous nature. Two samples from AGC Chemicals consisted of submicrometer particles in clusters (approximately 5 μm), while all the other samples consisted of larger micrometer-sized particles. Delay elements were prepared with 15/80/5 and 15/75/10 mixtures of $B_4C/NaIO_4$/PTFE using these samples. Differences in particle morphology had no discernible influence on the resulting IBR, while particle size did have an effect. At the 5 wt % PTFE level, the finest (submicrometer) samples gave distinctly slower-burning compositions (4.94 and 5.61 s/cm versus 3.4 s/cm for micrometer-sized PTFE). At the 10 wt % level, these samples gave highly packed columns (98−99% TMD) that did not ignite. It is well-known that mixtures of particles of greatly varying diameters readily form high-density compacts.[39,40]

CONCLUSIONS

In summary, we have shown that $B_4C/NaIO_4$/PTFE compositions may be used as pyrotechnic time delays. Inverse burning rates ranging from 1.3 to 20.8 s/cm were demonstrated in the hand-held signal delay housing, a heavy aluminum housing that readily quenches many other energetic systems. Burning times of 5−6 s, suitable for hand-held signals, were readily achieved. Composition stoichiometry and boron carbide particle size are the primary factors that govern burning rate.

Table 2. Effect of Varying B_4C Size[a]

entry	B_4C type (lot)	B_4C amount (wt %)	consolidated density (g/cm^3)	% TMD[b]	inverse burning rate (s/cm)	inverse burning rate (s/g)
1a	Alfa Aesar	15	3.095 (0.029)	92.02 (0.87)	4.52 (0.09)	8.24 (0.15)
2a	AEE 1500 grit	15	3.077 (0.010)	91.47 (0.29)	4.83 (0.04)	8.87 (0.08)
3a	AEE 1200 grit	15	3.116 (0.024)	92.65 (0.72)	5.10 (0.08)	9.24 (0.15)
4a	AEE 800 grit (A)	15	3.191 (0.027)	94.88 (0.80)	12.80 (0.30)	22.64 (0.59)
5a	AEE 800 grit (B)	15	3.140 (0.026)	93.36 (0.77)	32.1 (erratic)[c]	57.6 (erratic)[c]
6a	mixture[d]	15	3.174 (0.009)	94.36 (0.26)	10.66 (0.20)	18.95 (0.39)
1b	Alfa Aesar	20	2.971 (0.018)	90.38 (0.55)	3.00 (0.11)	5.69 (0.18)
2b	AEE 1500 grit	20	2.917 (0.023)	88.74 (0.70)	3.27 (0.06)	6.32 (0.12)
3b	AEE 1200 grit	20	2.934 (0.020)	89.26 (0.60)	3.32 (0.06)	6.38 (0.12)
4b	AEE 800 grit (A)	20	3.041 (0.027)	92.52 (0.82)	7.80 (0.13)	14.47 (0.17)
5b	AEE 800 grit (B)	20	2.998 (0.024)	91.20 (0.74)	18.09 (0.24)	34.06 (0.59)
6b	mixture[d]	20	2.996 (0.018)	91.13 (0.54)	5.93 (0.12)	11.18 (0.23)

[a]For compositions containing 15 or 20 wt % B_4C, 10 wt % AGC FL1650 PTFE, and −325 mesh $NaIO_4$ as the balance. All compositions were pressed at 376.6 MPa. Standard deviations for values are given in parentheses. [b]Consolidated density as a percentage of theoretical maximum. [c]Out of five samples tested, three did not ignite, one partially propagated, and one fully propagated with a burning time of 21.7 s. [d]A 50:50 mixture of Alfa Aesar and AEE 800 grit (B) was used.

The immense versatility of this system makes it promising for other applications in addition to hand-held signals. The development and application of environmentally benign and highly tunable pyrotechnic delay systems is an ongoing area of research in our laboratories.

■ ASSOCIATED CONTENT

Ⓢ Supporting Information

HHS housing and delay column configuration (Scheme S1); plots of mass-based IBR (s/g) and consolidated density (g/cm^3) for the experiments in Figures 1−3 (Figures S1−S3); particle size data for $NaIO_4$ samples (Table S1); effect of varying $NaIO_4$ size on consolidated density, % TMD, and IBR (Table S2); particle size and descriptive data for PTFE samples (Table S3); effect of varying PTFE type on consolidated density, and % TMD, and IBR (Table S4).This material is available free of charge via the Internet at http://pubs.acs.org.

■ AUTHOR INFORMATION

Corresponding Author

*Email: anthony.p.shaw.civ@mail.mil.

Author Contributions

The manuscript was written through contributions of all authors. All authors have given approval to the final version of the manuscript.

Notes

This document has been approved by the U.S. Government for public release; distribution is unlimited.

The authors declare no competing financial interest.

■ ACKNOWLEDGMENTS

The U.S. Army is thanked for funding this work through the RDECOM Environmental Quality Technology Program.

■ ABBREVIATIONS

ARDEC, Armament Research, Development and Engineering Center; HHS, hand-held signal; IBR, inverse burning rate; PFOA, perfluorooctanoic acid; PTFE, polytetrafluoroethylene; RDECOM, Research, Development and Engineering Command; VAAR, vinyl alcohol−acetate resin; % TMD, consolidated density as a percentage of theoretical maximum density

■ REFERENCES

(1) Tungsten Delay Composition, U.S. Military Specification MIL-T-23132A, June 16, 1972.

(2) Manganese Delay Composition, U.S. Military Specification MIL-M-21383A, October 22, 1976.

(3) Zirconium-Nickel Delay Composition, U.S. Military Specification MIL-C-13739A, November 15, 1965.

(4) T-10 Delay Composition, U.S. Military Specification MIL-D-85306A, November 7, 1991.

(5) Sellers, K.; Alsop, W.; Clough, S.; Hoyt, M.; Pugh, B.; Robb, J.; Weeks, K. *Perchlorate: Environmental Problems and Solutions*; CRC Press Taylor & Francis Group: Boca Raton, FL, 2007; Chapter 6, pp 131−148.

(6) *Chromium (VI) Handbook*; Guertin, J.; Jacobs, J. A.; Avakian, C. P., Eds.; CRC Press: Boca Raton, FL, 2004; Chapters 12−13, pp 491−564.

(7) Toxicological Profile for Barium, Chapter 8: Regulations and Advisories, U.S. Agency for Toxic Substances and Disease Registry. http://www.atsdr.cdc.gov/toxprofiles/tp24-c8.pdf (accessed May 29, 2013).

(8) Moretti, J. D.; Sabatini, J. J.; Shaw, A. P.; Chen, G.; Gilbert, R. A.; Oyler, K. D. Prototype scale development of an environmentally benign yellow smoke hand-held signal formulation based on solvent yellow 33. *ACS Sustainable Chem. Eng.* **2013**, *1*, 673−678.

(9) Sabatini, J. J.; Raab, J. M.; Hann, R. K.; Freeman, C. T. Brighter- and longer-burning barium-free illuminants for military and civilian pyrotechnics. *Z. Anorg. Allg. Chem.* **2013**, *639*, 25−30.

(10) Poret, J. C.; Shaw, A. P.; Csernica, C. M.; Oyler, K. D.; Estes, D. P. Development and performance of the W/Sb_2O_3/KIO_4/lubricant pyrotechnic delay in the U.S. Army hand-held signal. *Propellants, Explos., Pyrotech.* **2013**, *38*, 35−40.

(11) Saha, R.; Nandi, R.; Saha, B. Sources and toxicity of hexavalent chromium. *J. Coord. Chem.* **2011**, *64*, 1782−1806.

(12) *Chemistry of Arsenic, Antimony, and Bismuth*; Norman, N. C., Ed.; Thomson Science: London, 1998; Chapter 8, pp 403−440.

(13) De Ment, J. Composition for smoke production. U.S. Patent 2,995,526, August 8, 1961.

(14) Lane, G. A.; Smith, W. A.; Jankowiak, E. M. Novel Pyrotechnic Compositions for Screening Smokes. *Proceedings of the 1st International Pyrotechnics Seminar*; Estes Park, CO, U.S.A., August 12−16, 1968; pp 263−291.

(15) Lane, G. A.; Jankowiak, E. M.; Smith, W. A. *Techniques in Smoke Application*; Accession Number CBRNIAC-CB-136829; Defense Technical Information Center (DTIC): Fort Belvoir, VA, 1968; pp 1−64.

(16) Sabatini, J. J.; Poret, J. C.; Broad, R. N. Boron carbide as a barium-free green light emitter and burn-rate modifier in pyrotechnics. *Angew. Chem., Int. Ed.* **2011**, *50*, 4624−4626.

(17) Shaw, A. P.; Poret, J. C.; Gilbert, R. A.; Moretti, J. D.; Sabatini, J. J.; Oyler, K. D.; Chen, G. Pyrotechnic Smoke Compositions Containing Boron Carbide. *Proceedings of the 38th International Pyrotechnics Seminar*; Denver, CO, U.S.A., June 10−15, 2012; pp 569−582.

(18) Shaw, A. P.; Poret, J. C.; Gilbert, R. A.; Domanico, J. A.; Black, E. L. Development and performance of boron carbide-based smoke compositions. *Propellants, Explos., Pyrotech.* **2013**, DOI: 10.1002/prep.201200166.

(19) Moretti, J. D.; Sabatini, J. J.; Chen, G. Periodate salts as pyrotechnic oxidizers: Development of barium- and perchlorate-free incendiary formulations. *Angew. Chem., Int. Ed.* **2012**, *51*, 6981−6983.

(20) The ionic radii of I^-, ClO_4^-, and IO_4^- are 220 pm, 240 pm, and 249 pm, respectively. Marcus, Y. *Ion Properties*; CRC Press: Boca Raton, FL, 1997; pp 44−62.

(21) Koch, E.-C. *Metal-Fluorocarbon Based Energetic Materials*; Wiley-VCH Verlag & Co.: Weinheim, Germany, 2012; pp 42−67.

(22) Klapötke, T. M. *Chemistry of High-Energy Materials*, 2nd ed.; Walter de Gruyter: Berlin/New York, 2012; pp 65−70.

(23) Lau, C.; Anitole, K.; Hodes, C.; Lai, D.; Pfahles-Hutchens, A.; Seed, J. Perfluoroalkyl acids: A review of monitoring and toxicological findings. *Toxicol. Sci.* **2007**, *99*, 366−394.

(24) 2012 Annual Progress Report, 2010/15 PFOA Stewardship Program, U.S. Environmental Protection Agency. http://www.epa.gov/oppt/pfoa/pubs/stewardship/preports6.html (accessed May 24, 2013).

(25) Ebnesajjad, S. *Introduction to Fluoropolymers: Materials, Technology, and Applications*; Elsevier: Amsterdam, 2013; pp 98−100.

(26) Comyn, R. H. *Pyrotechnic Research at DOFL, Part II: Pyrotechnic Delays*; Accession Number AD0273042; Defense Technical Information Center (DTIC): Fort Belvoir, VA, 1962; pp 1−39.

(27) Valenta, F. J. The State-of-the-Art of Navy Pyrotechnic Delays. *Proceedings of the 3rd International Pyrotechnics Seminar*; Colorado Springs, CO, U.S.A., August 21−25, 1972; pp 185−195.

(28) Valenta, F. J. Some Factors Affecting Burning Rates and Variability of Tungsten and Manganese Delay Compositions. *Proceedings of the 3rd International Pyrotechnics Seminar*; Colorado Springs, CO, U.S.A., August 21−25, 1972; pp 157−183.

(29) Brown, M. E.; Rugunanan, R. A. A temperature-profile study of the combustion of black powder and its constituent binary mixtures. *Propellants, Explos., Pyrotech.* **1989**, *14*, 69−75.

(30) Domnich, V.; Reynaud, S.; Haber, R. A.; Chhowalla, M. Boron carbide: Structure, properties, and stability under stress. *J. Am. Ceram. Soc.* **2011**, *94*, 3605−3628.
(31) *CRC Handbook of Chemistry and Physics*, 85th ed.; Lide, D. R., Ed.; CRC Press: Boca Raton, FL, 2004; Section 4, pp 37−96.
(32) Clark, E. S. The molecular conformations of polytetrafluoroethylene: Forms II and IV. *Polymer* **1999**, *40*, 4659−4665.
(33) Domalski, E. S.; Armstrong, G. T. The heat of formation of boron carbide. *J. Res. Natl. Bur. Stand., Sect. A* **1968**, *72A*, 133−139.
(34) Li, Y. Q.; Qiu, T. Oxidation behaviour of boron carbide powder. *Mater. Sci. Eng., A* **2007**, *444*, 184−191.
(35) Wood, C.; Emin, D.; Gray, P. E. Thermal conductivity of boron carbides. *Phys. Rev. B* **1985**, *31*, 6811−6814.
(36) Conkling, J. A.; Mocella, C. J. *Chemistry of Pyrotechnics: Basic Principles and Theory*, 2nd ed.; CRC Press Taylor & Francis Group: Boca Raton, FL, 2011; pp 163−168.
(37) Wilson, M. A.; Hancox, R. J. Pyrotechnic Delays and Thermal Sources. In *Pyrotechnic Chemistry: Pyrotechnic Reference Series No. 4*; Journal of Pyrotechnics, Inc.: Whitewater, CO, 2004; Chapter 8, pp 1−22.
(38) McLain, J. H. *Pyrotechnics: From the Viewpoint of Solid State Chemistry*; The Franklin Institute Press: Philadelphia, PA, 1980; pp 46−62.
(39) Hudson, D. R. Density and packing in an aggregate of mixed spheres. *J. Appl. Phys.* **1949**, *20*, 154−162.
(40) McGeary, R. K. Mechanical packing of spherical particles. *J. Am. Ceram. Soc.* **1961**, *44*, 513−522.

Supporting Information

Versatile Boron Carbide-Based Energetic Time Delay Compositions

Jay C. Poret, Anthony P. Shaw, Christopher M. Csernica, Karl D. Oyler, Jessica A. Vanatta, Gary Chen*

Armament Research, Development and Engineering Center,
US Army RDECOM-ARDEC, Picatinny Arsenal, NJ 07806, USA
*email: anthony.p.shaw.civ@mail.mil

Contents:

Scheme S1. HHS delay housing and delay column configuration. S2

Figure S1. Mass-based IBR and consolidated densities for experiments in Figure 1. S3

Figure S2. Mass-based IBR and consolidated densities for experiments in Figure 2. S4

Figure S3. Mass-based IBR and consolidated densities for experiments in Figure 3. S5

Table S1. Particle size data for $NaIO_4$ samples. S6

Table S2. Effect of varying $NaIO_4$ size. S6

Table S3. Particle size and descriptive data for PTFE samples. S7

Table S4. Effect of varying PTFE type. S7

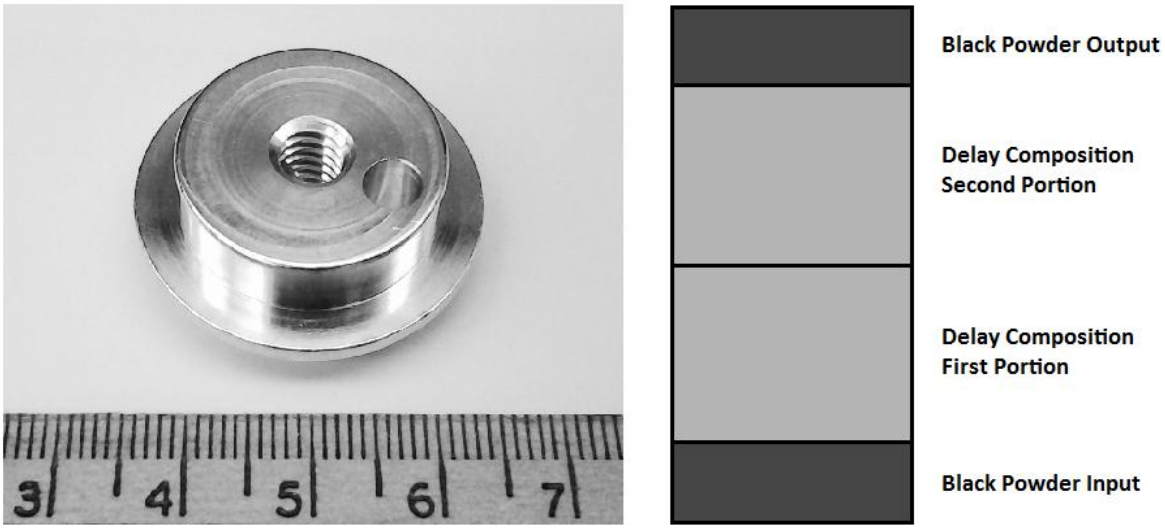

Scheme S1. HHS delay housing and delay column configuration. The delay column and black powder layers occupy the off-center 4.8 mm diameter cavity.

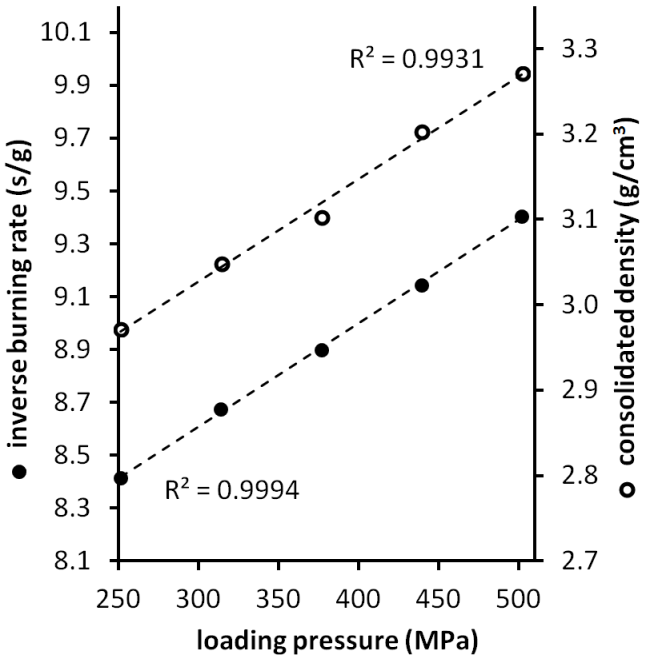

Figure S1. Inverse burning rate (s/g, closed circles) and consolidated density (g/cm^3, open circles) as functions of loading pressure. Data is shown for a 15/75/10 mixture of B_4C/$NaIO_4$/PTFE. AEE 1500 grit B_4C, −325 mesh $NaIO_4$, and AGC FL1650 PTFE were used.

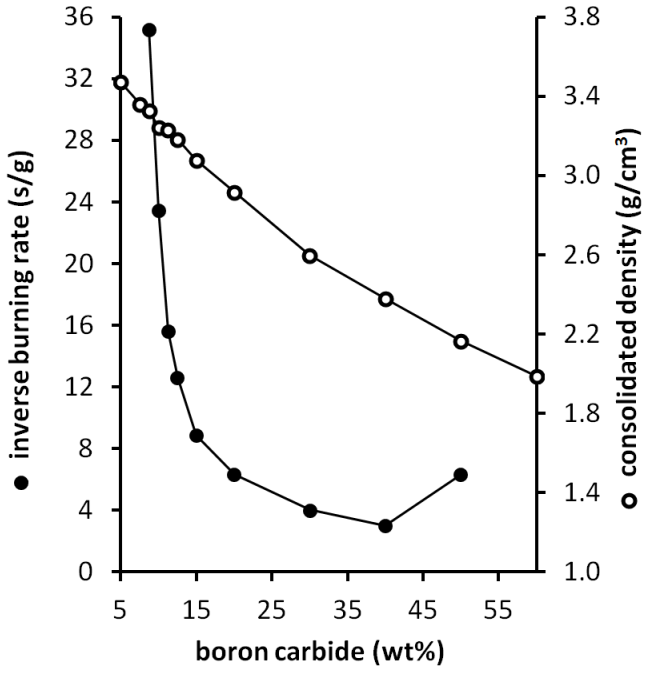

Figure S2. Inverse burning rates (s/g, closed circles) and consolidated densities (g/cm^3, open circles) for x/(90−x)/10 mixtures of B_4C/$NaIO_4$/PTFE. Data is shown for compositions containing AEE 1500 grit B_4C, −325 mesh $NaIO_4$, and AGC FL1650 PTFE. All compositions were pressed at 376.6 MPa.

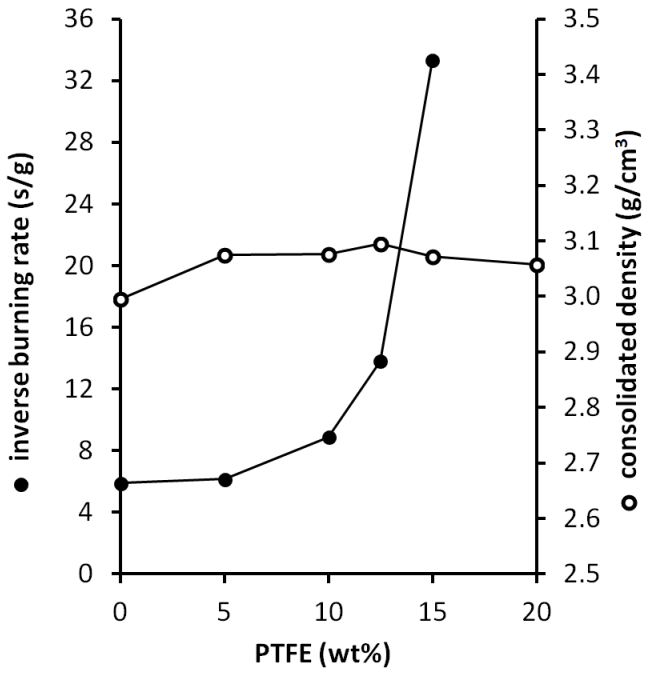

Figure S3. Inverse burning rates (s/g, closed circles) and consolidated densities (g/cm^3, open circles) for 15/(85−*x*)/*x* mixtures of B_4C/$NaIO_4$/PTFE. Data is shown for compositions containing AEE 1500 grit B_4C, −325 mesh $NaIO_4$, and AGC FL1650 PTFE. All compositions were pressed at 376.6 MPa.

Table S1. Particle size data for $NaIO_4$ samples.

Mesh Fraction [a]	D[4,3] [b]	D[v, 0.1] [c]	D[v, 0.5] [c]	D[v, 0.9] [c]
−325	52.09	25.82	46.22	76.46
−200	59.43	25.48	54.76	92.83
−200, +325	83.27	60.46	80.31	108.0
−80, +200	149.6	105.2	141.6	203.9

a) $NaIO_4$ fractions obtained by screening. b) Volume-based mean diameter in μm. c) D[v, *x*] is the diameter in μm that (100·*x*)% of the volume distribution is below.

Table S2. Effect of varying $NaIO_4$ size. [a]

Entry	$NaIO_4$ Mesh Fraction	B_4C Amount (wt%)	Consolidated Density (g/cm^3)	%TMD [b]	Inverse Burning Rate (s/cm)	Inverse Burning Rate (s/g)
1a	−325	15	3.077 (0.010)	91.47 (0.29)	4.83 (0.04)	8.87 (0.08)
2a	−200	15	3.136 (0.013)	93.24 (0.38)	5.04 (0.03)	9.06 (0.04)
3a	−200, +325	15	3.169 (0.011)	94.22 (0.32)	5.59 (0.04)	9.95 (0.08)
4a	−80, +200	15	3.220 (0.028)	95.74 (0.83)	6.16 (0.06)	10.80 (0.11)
1b	−325	20	2.917 (0.023)	88.74 (0.70)	3.27 (0.06)	6.32 (0.12)
2b	−200	20	2.959 (0.019)	90.02 (0.58)	3.37 (0.08)	6.43 (0.12)
3b	−200, +325	20	2.970 (0.009)	90.34 (0.27)	3.70 (0.05)	7.02 (0.08)
4b	−80, +200	20	3.011 (0.030)	91.60 (0.90)	4.33 (0.04)	8.12 (0.11)

a) For compositions containing 15 or 20 wt% AEE 1500 grit B_4C, 10 wt% AGC FL1650 PTFE, and $NaIO_4$ as the balance. All compositions were pressed at 376.6 MPa. Standard deviations for values are given in parentheses. b) Consolidated density as a percentage of theoretical maximum.

Table S3. Particle size and descriptive data for PTFE samples. [a)]

PTFE Type	Description	Bulk Density (g/L)	D[v, 0.1] [b)]	D[v, 0.5] [b)]	D[v, 0.9] [b)]
AGC TL-171E	clusters of rounded sub-micron particles	431	1.4	5.2	15.9
AGC FL1710	clusters of rounded sub-micron particles	444	1.5	5.7	16.5
AGC FL1690	irregular shape ~16 μm [c)]	432	6.3	32.8	78.0
AGC TL-368	irregular shape slightly fibrous ~12 μm [c)]	404	13.5	42.5	101.5
AGC FL1650	rounded ~17 μm [c)]	451	13.9	44.1	108.8
DuPont 7C	irregular shape extremely fibrous ~28 μm [d)]	250	-	-	-

a) Manufacturer data. b) Laser diffraction data, D[v, *x*] is the diameter in μm that (100·*x*)% of the volume distribution is below. c) Size by Hegman ASTM D1210. d) Average particle size by ASTM D4894.

Table S4. Effect of varying PTFE type. [a)]

Entry	PTFE Type	PTFE Amount (wt%)	Consolidated Density (g/cm^3)	%TMD [b)]	Inverse Burning Rate (s/cm)	Inverse Burning Rate (s/g)
1a	AGC TL-171E	5	3.211 (0.017)	92.63 (0.49)	4.94 (0.05)	8.68 (0.12)
2a	AGC FL1710	5	3.192 (0.017)	92.10 (0.49)	5.61 (0.04)	9.91 (0.03)
3a	AGC FL1690	5	3.114 (0.015)	89.84 (0.43)	3.39 (0.03)	6.14 (0.05)
4a	AGC TL-368	5	3.123 (0.020)	90.10 (0.58)	3.39 (0.01)	6.12 (0.05)
5a	AGC FL1650	5	3.075 (0.013)	88.72 (0.38)	3.35 (0.03)	6.15 (0.05)
6a	DuPont 7C	5	3.088 (0.018)	89.09 (0.52)	3.43 (0.05)	6.27 (0.07)
1b [c)]	AGC TL-171E	10	3.300 (0.011)	98.10 (0.33)	-	-
2b [c)]	AGC FL1710	10	3.335 (0.021)	99.16 (0.62)	-	-
3b	AGC FL1690	10	3.131 (0.019)	93.07 (0.57)	5.41 (0.12)	9.74 (0.22)
4b	AGC TL-368	10	3.151 (0.016)	93.68 (0.48)	5.78 (0.09)	10.35 (0.21)
5b	AGC FL1650	10	3.077 (0.010)	91.47 (0.29)	4.83 (0.04)	8.87 (0.08)
6b	DuPont 7C	10	3.101 (0.020)	92.21 (0.60)	4.88 (0.07)	8.89 (0.13)

a) For compositions containing 15 wt% AEE 1500 grit B_4C, 5 or 10 wt% PTFE, and −325 mesh $NaIO_4$ as the balance. All compositions were pressed at 376.6 MPa. Standard deviations for values are given in parentheses. b) Consolidated density as a percentage of theoretical maximum. c) Did not ignite.